Small anisotropy, weak thermal fluctuations, and high field superconductivity in Co-doped iron pnictide $Ba(Fe_{1-x}Co_x)_2As_2$

A. Yamamoto,[1,a)] J. Jaroszynski,[1] C. Tarantini,[1] L. Balicas,[1] J. Jiang,[1] A. Gurevich,[1] D. C. Larbalestier,[1] R. Jin,[2] A. S. Sefat,[2] M. A. McGuire,[2] B. C. Sales,[2] D. K. Christen,[2] and D. Mandrus[2]

[1]*National High Magnetic Field Laboratory, Florida State University, Tallahassee, Florida 32310, USA*
[2]*Materials Science and Technology Division, Oak Ridge National Laboratory, Oak Ridge, Tennessee 37831, USA*

(Received 2 October 2008; accepted 25 January 2009; published online 13 February 2009)

We performed high-field magnetotransport and magnetization measurements on a single crystal of the 122-phase iron pnictide $Ba(Fe_{1-x}Co_x)_2As_2$. Unlike the high-temperature superconductor cuprates and 1111-phase oxypnictides, $Ba(Fe_{1-x}Co_x)_2As_2$ showed practically no broadening of the resistive transitions under magnetic fields up to 45 T. We report the temperature dependencies of the upper critical field H_{c2} both parallel and perpendicular to the *c*-axis, the irreversibility field $H_{irr}^{c}(T)$, and a rather unusual symmetric volume pinning force curve $F_p(H)$ suggestive of a strong pinning nanostructure. The anisotropy parameter $\gamma=H_{c2}^{ab}/H_{c2}^{c}$ deduced from the slopes of $dH_{c2}^{ab}/dT=4.9$ T/K and $dH_{c2}^{c}/dT=2.5$ T/K decreases from ~2 near T_c, to ~1.5 at lower temperatures, much smaller than γ for 1111pnictides and high-T_c cuprates. © *2009 American Institute of Physics*. [DOI: 10.1063/1.3081455]

The discovery of superconductivity in iron oxypnictides[1] has attracted strong interest due to an unusual interplay of superconductivity and magnetism and extremely high upper critical fields H_{c2}.[2,3] Like the high temperature superconductor (HTS) cuprates, iron pnictides are layered with alternating basal Fe-As layers sandwiched between doped charge reservoir layers. Superconductivity appears upon doping a parent antiferromagnetic state with electrons[1,4] or holes,[5] resulting in high transition temperatures T_c up to 55 K for the 1111 type single layer oxypnictides REFeAsO (RE denotes rare earth). The recently discovered 122 type $AEFe_2As_2$ compounds (AE denotes alkali or alkali earth) become superconducting with T_c up to 38 K by hole doping.[6] Electron doping induced by substituting Co (Ref. 7) or Ni (Ref. 8) for Fe can also induce superconductivity, but, unlike the cuprates, iron pnictides can tolerate magnetic impurities in the superconducting layers.

Our previous high-field measurements on the La, Nd, and Sm 1111 iron oxypnictides showed very high upper critical fields H_{c2} of ~65 T for $LaFeAsO_{1-x}F_x$ polycrystals[2] and even greater than 100 T for Nd and Sm pnictides.[3] However, the Nd and Sm 1111 compounds exhibit field-induced, thermally activated broadening of the resistive transitions reminiscent of that in the cuprates. Concurrently, quasireversible magnetization was observed in $LaFeAsO_{1-x}F_x$ polycrystals, indicative of weak pinning of a nearly equilibrium vortex lattice.[9] It was also suggested that the higher-T_c oxypnictides, like the cuprates, may have a grain boundary weak-link problem.[9–11] On the other hand, the 122 pnictides have lower T_c but also much lower anisotropy than the 1111 oxypnictides.[12–14] Here, we report on $H_{c2}(T)$ and the irreversibility field $H_{irr}(T)$ in $Ba(Fe,Co)_2As_2$ single crystals. Surprisingly, we found conventional low-temperature-superconductor-like (LTS) displacements of the resistive transition in fields up to 45 T, indications for strong vortex pinning, and a very high H_{irr} close to the onset of the superconducting transition at H_{c2}. Both H_{c2} and H_{irr} exceed the BCS paramagnetic limit at low *T*.

Cobalt-doped $BaFe_2As_2$ single crystals were synthesized by the self-flux method.[7] The present $Ba(Fe_{0.9}Co_{0.1})_2As_2$ crystal has dimensions of $1.28\times0.58\times0.030$ mm^3. High field magnetotransport measurements were performed using the National High Magnetic Field Laboratory DC 45 T hybrid magnet and a 16 T Quantum Design physical property measurement system. The full critical state magnetization was measured in an Oxford 14 T vibrating sample magnetometer.

Our crystal has T_c of 22 K inferred from the susceptibility measurements. Figure 1 shows magnetization hysteresis loops which exhibit a small "fish-tail" hump at 5–10 T, similar to that of $(Ba,K)Fe_2As_2$ [15] and $YBa_2Cu_3O_{7-\delta}$ crystals.[16]

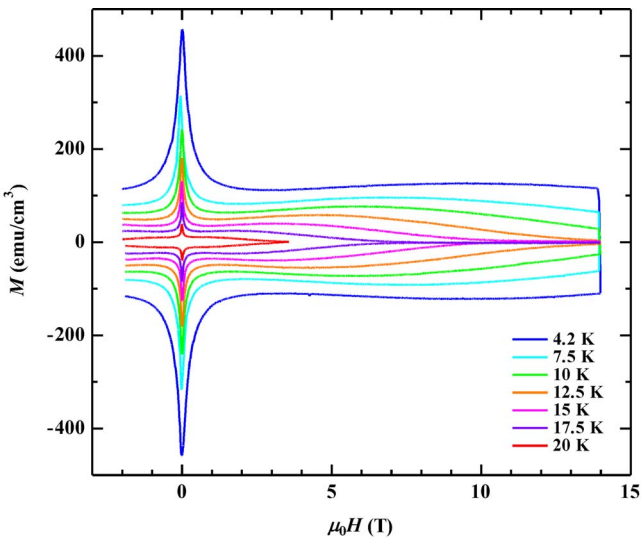

FIG. 1. (Color online) Magnetization hysteresis loops at 4.2, 7.5, 10, 12.5, 15, 17.5, and 20 K. Magnetic field was applied parallel to *c*-axis.

a)Electronic mail: yamamoto@asc.magnet.fsu.edu.

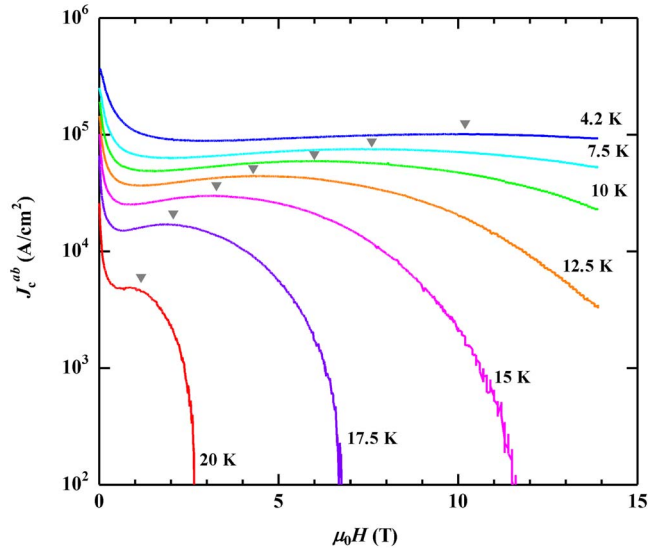

FIG. 2. (Color online) Magnetic field dependence of the in-plane critical current density J_c. Triangles indicate broad maximum positions.

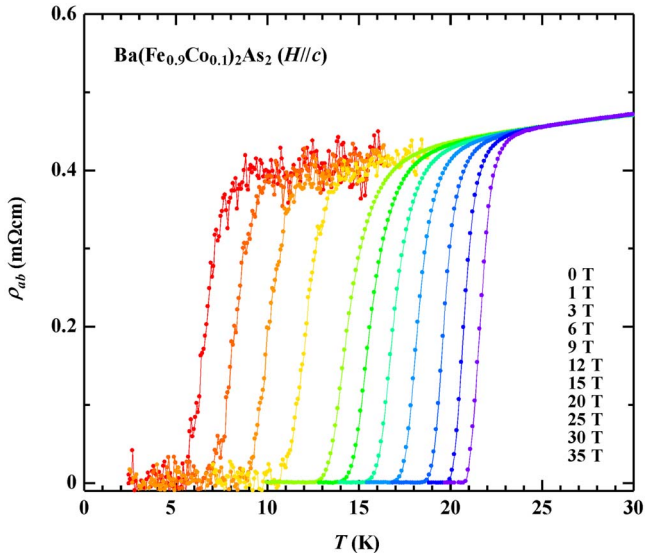

FIG. 4. (Color online) In-plane resistivity ρ_{ab} as a function of temperatures under magnetic field of $\mu_0 H$=0, 1, 3, 6, 9, 12, 15, 20, 25, 30, and 35 T. High field measurements above 15 T was performed using 45 T hybrid magnet.

The critical current density J_c calculated from the width of the hysteresis loops using the Bean model is shown in Fig. 2. J_c exhibits a rapid decrease at low fields followed by broad maxima and a relatively weak field dependence at high-fields. The self-field $J_c \simeq 4\times 10^5$ A/cm^2 at 4.2 K is indeed high for a single crystal.

To assess mechanisms, which control the vortex pinning force $F_p=\mu_0 H J_c$, we plot in Fig. 3 the normalized pinning force $F_p/F_p^{\max}$ as a function of the reduced field $h=H/H_{\rm irr}$. Here we define the irreversibility field $H_{\rm irr}$ at which $J_c(H)$ extrapolates to zero from the field closure of hysteretic magnetization loops. The normalized curves of $F_p(h,T)$ for $T>15$ K and $(0.05-0.1)<h<1$ collapse into a single curve described by the scaling function $h^p(1-h)^q$ with $p=1.67$ and $q=2$ (Ref. 17). Moreover, the lower T and partial $F_p(h)$ curves taken at 4.2–12.5 K also exhibit the same field dependence, allowing $H_{\rm irr}$ to be estimated down to $\sim$10 K. The observed F_p scaling, which is independent of temperature, suggests one dominant vortex pinning mechanism, while the symmetric $F_p(h)$ curves with a peak at $h\sim 0.45$ imply a dense vortex pinning nanostructure, perhaps resulting from an inhomogeneous distribution of cobalt ions, which produces a locally varying order parameter. This scenario is consistent with a spatial variation of K in (Ba,K)Fe$_2$As$_2$ single crystals[18] and similar to the field-induced pinning by oxygen deficient regions in YBa$_2$Cu$_3$O$_{7-\delta}$.[16]

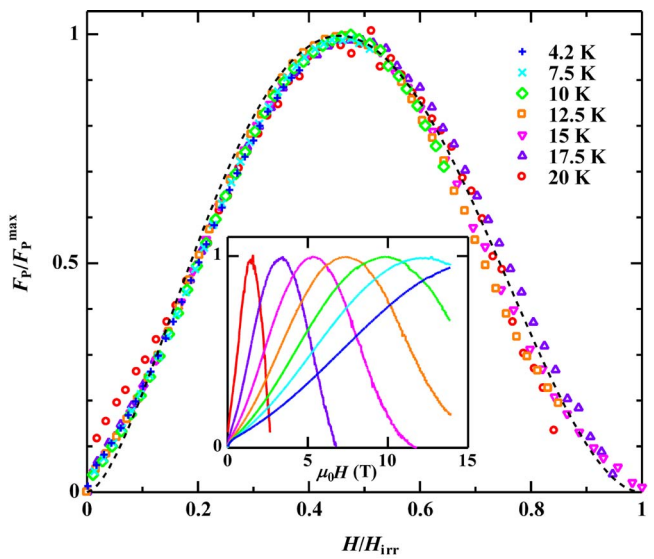

FIG. 3. (Color online) Normalized flux pinning force $F_p/F_p^{\max}$ as a function of reduced field $h=H/H_{\rm irr}$. Dashed line represents the fitting curve $h^{1.67}(1-h)^2$. Inset shows $F_p/F_p^{\max}$ as a function of field H.

The results of magnetotransport measurements in fields parallel to the c-axis up to 45 T are shown in Fig. 4. It is clear that the $R(T)$ curves are displaced to lower temperatures upon increasing fields, but also that they do not noticeably broaden. The transition widths ΔT defined by the 90% and 10% points on $R(T)$ do not exceed 2–3 K. The transitions with fields parallel to the ab plane were similarly sharp up to 45 T. This lack of broadening of the resistive transitions under field is in strong contrast to some of the 1111 oxypnictides[2,3,19] and rather similar to a conventional LTS like Nb$_3$Sn.[20]

The combined high field magneto transport and magnetization analyses enable us to obtain the magnetic phase diagram. The temperature-dependent resistive $H_{c2}(T)$ defined by 90% of R_n is shown in Fig. 5. Both H_{c2}^{ab} and H_{c2}^{c} exhibit almost linear temperature dependence near T_c with slopes of $dH_{c2}^{ab}/dT=4.9$ T/K and $dH_{c2}^{c}/dT=2.5$ T/K. The anisotropy $\gamma=H_{c2}^{ab}/H_{c2}^{c}$ varies from $\sim$1.5 to 2 as T increases (see inset of Fig. 5). This temperature-dependent γ is consistent with multiband superconductivity, however $\gamma=1.5-2$ is significantly lower than $\gamma=5-10$ measured on the 1111 oxypnictides.[3,21,22] The low temperature H_{c2} extrapolates to >60 T, much larger than the Werthamer–Helfand–Hohenberg extrapolation $H_{c2}^{c}(0)\sim 0.69 T_c |dH_{c2}/dT|_{Tc}$ $\sim$38 T, indicating unconventional $H_{c2}(T)$ behavior. Moreover, even at $T=T_c/2$, the observed H_{c2}^{ab} already exceeds the BCS paramagnetic limit $H_p[T]=1.84T_c[K]\sim 40.5$ T. Extrapolations of the $H_{c2}(T)$ data in Fig. 5 suggest $H_{c2}^{ab}(0)$ $\sim$70 T and $H_{c2}^{c}(0)\sim 50$ T, comparable to the estimates of $\sim$70 T for (Ba,K)Fe$_2$As$_2$ (Refs. 12–14) and $\sim$65 T for the optimally doped LaFeAsO$_{0.89}$F$_{0.11}$,[2,19] though much smaller than $H_{c2}(0)>100$ T for Nd and Sm oxypnictides.[3]

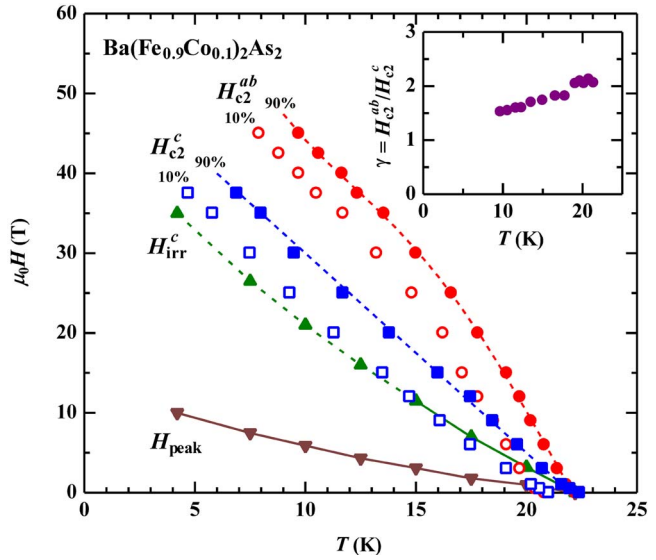

FIG. 5. (Color online) Magnetic phase diagram of the $Ba(Fe_{0.9}Co_{0.1})_2As_2$ single crystal. Filled and open symbols represent $H(T)$ defined by $R(T,H)=0.9R_n$ and $R(T,H)=0.1R_n$, respectively. Circles and squares represent resistive H_{c2} parallel to the *ab* plane and *c*-axis, respectively. Upward-pointing triangles represent the irreversibility field H_{irr}^{c} extrapolated from the pining force curves shown in Fig. 3. For $H_{irr}>14$ T, H_{irr} was estimated from the scaling of F_p curves as described in the text. Downward-pointing triangles mark the field of the fish-tail peaks on magnetic hysteresis loops. The temperature dependencies of H_{irr} and the field of the fish-tail magnetization peak can be fitted with $H^*=H^*(0)\times(1-T/T_c)^{5/4}$. Inset shows the temperature dependence of H_{c2} anisotropy parameter $\gamma=H_{c2}^{ab}/H_{c2}^{c}$.

Now we discuss the relationship of H_{c2} and H_{irr} defined conventionally as the field at which $J_c(H)$ extrapolates to zero, which gives $H_{irr}(T)$ close to the onset of the flux flow resistance at $R(T)=0.1R_n$. The lack of the field-induced broadening of $R(T)$ and the fact that H_{c2} and H_{irr} are not very different indicate the LTS-like behavior, unlike HTS cuprates in which H_{irr} is well below H_{c2} due to strong thermal fluctuations of vortices. This LTS-like behavior is also consistent with weak thermal fluctuations, as follows from the estimation of the Ginzburg number[23] $Gi=(2\pi k_B T_c \mu_0 \lambda_0^2/\Phi_0^2 \xi_c)^2/2 \sim 6.8\times10^{-5}$, much lower than for the least anisotropic cuprate $YBa_2Cu_3O_{7-\delta}$ $(\sim10^{-2})$ and the polycrystalline NdFeAs(O,F) and $SmFeAsO_{1-\delta}$ $(\sim10^{-2})$, and the LaFeAs(O,F) $(\sim3.4\times10^{-4})$,[3] and even for clean MgB_2 $(\sim2.0\times10^{-4})$. Here the London penetration depths $\lambda_{ab}=160$ nm and $\lambda_c\sim\gamma\lambda_{ab}=320$ nm were estimated from the lower critical field $H_{c1}^{ab}\sim\Phi_0(\ln\kappa+0.5)/4\pi\lambda_{ab}\lambda_c$ measured from the deviation of the diamagnetic magnetization using a superconducting quantum interference device magnetometer, where $\kappa\sim65$ is the Ginzburg–Landau parameter. $H_{c1}(T)$ show the usual linear temperature dependence with $dH_{c1}^{ab}/dT=0.79$ mT/K near T_c, extrapolating to $H_{c1}^{ab}(0)\sim15$ mT. The coherence lengths $\xi_{ab}=2.44$ nm and $\xi_c\sim\gamma^{-1}\xi_{ab}=1.22$ nm were evaluated from $H_{c2}(0)$.

Given the weakness of vortex thermal fluctuations, the finite width of $R(T)$ in our single crystal likely results from random T_c inhomogeneities due to local compositional variations, proximity effect near defects, etc., which cause local fluctuations of H_{c2} and the flux flow resistivity so that the curve $R(T)$ reflects the percolative transition in a weakly inhomogeneous superconductor. In this case the onset of the superconducting transition at H_{c2} represents the maximum H_{c2}. In turn, the onset of the global magnetic irreversibility at H_{irr} may be interpreted as the field percolation threshold at which the lower H_{c2} superconducting regions form an infinite percolation cluster.

In summary, our magnetization and transport measurements show very high H_{c2} exceeding the BCS paramagnetic limit, and lack of field-induced broadening of the resistive transitions up to 45 T. The irreversibility field H_{irr} is close to H_{c2}, indicating weak thermal fluctuations and/or strong vortex pinning. Thus, Co-doped 122 pnictide is a quasi-LTS high field superconductor with $H_{c2}>50$ T and a weak anisotropy with $\gamma<2$.

Work at the NHMFL was supported by the NSF Cooperative Agreement DMR-0084173, by the State of Florida, by the DOE and by AFOSR under Grant No. FA9550-06-1-0474. Work at ORNL was supported by the Division of Materials Science and Engineering, Office of Basic Energy Sciences. AY is supported by a fellowship of the JSPS.

[1] Y. Kamihara, T. Watanabe, M. Hirano, and H. Hosono, J. Am. Chem. Soc. **130**, 3296 (2008).
[2] F. Hunte, J. Jaroszynski, A. Gurevich, D. Larbalestier, R. Jin, A. Sefat, M. McGuire, B. Sales, D. Christen, and D. Mandrus, Nature (London) **453**, 903 (2008).
[3] J. Jaroszynski *et al.*, Phys. Rev. B **78**, 064511 (2008); **78**, 174523 (2008).
[4] A. S. Sefat, M. A. McGuire, B. C. Sales, R. Jin, J. Y. Howe, and D. Mandrus, Phys. Rev. B **77**, 174503 (2008).
[5] H. H. Wen, G. Mu, L. Fang, H. Yang, and X. Zhu, Europhys. Lett. **82**, 17009 (2008).
[6] M. Rotter, M. Tegel, and D. Johrendt, Phys. Rev. Lett. **101**, 107006 (2008).
[7] A. S. Sefat, R. Jin, M. A. McGuire, B. C. Sales, D. J. Singh, and D. Mandrus, Phys. Rev. Lett. **101**, 117004 (2008).
[8] L. J. Li, Q. B. Wang, Y. K. Luo, H. Chen, Q. Tao, Y. K. Li, X. Lin, M. He, Z. W. Zhu, G. H. Cao, and Z. A. Xu, arXiv:0809.2009v2.
[9] A. Yamamoto, J. Jiang, C. Tarantini, N. Craig, A. Polyanskii, F. Kametani, F. Hunte, J. Jaroszynski, E. Hellstrom, D. Larbalestier, R. Jin, A. Sefat, M. McGuire, B. Sales, D. Christen, and D. Mandrus, Appl. Phys. Lett. **92**, 252501 (2008).
[10] R. Prozorov, M. E. Tillman, E. D. Mun, and P. C. Canfield, arXiv:0805.2783v2.
[11] A. Yamamoto, A. Polyanskii, J. Jiang, F. Kametani, C. Tarantini, F. Hunte, J. Jaroszynski, E. Hellstrom, P. Lee, A. Gurevich, D. Larbalestier, Z. Ren, J. Yang, X. Dong, W. Lu, and Z. Zhao, Supercond. Sci. Technol. **21**, 095008 (2008).
[12] H. Q. Yuan, J. Singleton, F. F. Balakirev, G. F. Chen, J. L. Luo, and N. L. Wang, Nature (London) **457**, 565 (2009).
[13] M. Altarawneh, K. Collar, C. Mielke, N. Ni, S. Bud'ko, and P. Canfield, Phys. Rev. B **78**, 220505 (2008).
[14] Z. S. Wang, H. Q. Luo, C. Ren, and H. H. Wen, Phys. Rev. B **78**, 140501(R) (2008).
[15] H. Yang, H. Luo, Z. Wang, and H. H. Wen, Appl. Phys. Lett. **93**, 142506 (2008).
[16] M. Daeumling, J. Seuntjens, and D. Larbalestier, Nature (London) **346**, 332 (1990).
[17] E. J. Kramer, J. Appl. Phys. **44**, 1360 (1973).
[18] N. Ni, S. Nandi, A. Kreyssig, A. I. Goldman, E. D. Mun, S. L. Bud'ko, and P. C. Canfield, Phys. Rev. B **78**, 014523 (2008).
[19] Y. Kohama, Y. Kamihara, S. A. Baily, L. Civale, S. C. Riggs, F. F. Balakirev, T. Atake, M. Jaime, M. Hirano, and H. Hosono, arXiv:0809.1133v2.
[20] A. Godeke, M. Jewell, C. Fischer, A. Squitieri, P. Lee, and D. Larbalestier, J. Appl. Phys. **97**, 093909 (2005).
[21] U. Welp, R. Xie, A. E. Koshelev, W. K. Kwok, P. Cheng, L. Fang, and H. H. Wen, Phys. Rev. B **78**, 140510(R) (2008).
[22] L. Balicas, A. Gurevich, Y. J. Jo, J. Jaroszynski, D. C. Larbalestier, R. H. Liu, H. Chen, X. H. Chen, N. D. Zhigadlo, S. Katrych, Z. Bukowski, and J. Karpinski, arXiv:0809.4223v1.
[23] G. Blatter, M. V. Feigel'man, V. B. Geshkenbein, A. I. Larkin, and V. M. Vinokur, Rev. Mod. Phys. **66**, 1125 (1994).